

Article

Modified Electrode with ZnO Nanostructures Obtained from Silk Fibroin for Amoxicillin Detection

Cristina Dumitriu , Alexandra Constantinescu, Alina Dumitru and Cristian Pirvu * 

Faculty of Chemical Engineering and Biotechnologies, Politehnica University of Bucharest, 1-7 Polizu Street, 011061 Bucharest, Romania

* Correspondence: cristian.pirvu@upb.ro; Tel.: +40-214-023-930; Fax: +40-213-111-796

Abstract: Antibiotics are a novel class of contaminants that represent a substantial risk to human health, making their detection an important task. In this study, ZnO nanostructures were prepared starting from *Bombyx mori* silk fibroin and $\text{Zn}(\text{NO}_3)_2$, using thermal treatment. The resulting ZnO structures were characterized using SEM, FT-IR, and XRD. They had a fibrous morphology with a wurtzite crystalline structure, with nanometric dimensions. FT-IR and XRD confirmed silk fibroin's disappearance after thermal treatment. To prepare modified electrodes for amoxicillin (AMX) antibiotic detection, ZnO nanostructures were mixed with Nafion polymer and drop-casted on an electrode's surface. Parameters such as drying time and concentration appeared to be important for electrochemical detection. Differential pulse voltammetry (DPV) was sensitive for AMX detection. The measurements revealed that the novel electrode based on ZnO nanostructures embedded in Nafion polymer has potential to be used for AMX electrochemical detection.

Keywords: nanostructures; silk fibroin; electrochemical sensor



Citation: Dumitriu, C.;

Constantinescu, A.; Dumitru, A.;

Pirvu, C. Modified Electrode with ZnO Nanostructures Obtained from Silk Fibroin for Amoxicillin Detection. *Crystals* **2022**, *12*, 1511. <https://doi.org/10.3390/cryst12111511>

Academic Editors: Andrew F. Zhou and Peter X. Feng

Received: 20 September 2022

Accepted: 23 October 2022

Published: 25 October 2022

Publisher's Note: MDPI stays neutral with regard to jurisdictional claims in published maps and institutional affiliations.



Copyright: © 2022 by the authors. Licensee MDPI, Basel, Switzerland. This article is an open access article distributed under the terms and conditions of the Creative Commons Attribution (CC BY) license (<https://creativecommons.org/licenses/by/4.0/>).

1. Introduction

One of the most frequently prescribed antibiotics for infectious diseases that can affect humans (such as Anthrax, Lyme disease, pneumonia, gastroenteritis, otitis, vaginal infections, urinary infections, and oral infections) is amoxicillin (AMX) [1,2]. AMX, 6-(p-hydroxy- α -amino phenyl acetoamido) penicillanic acid [3], is also a common antibiotic used in animal husbandry, and because of this, its residues may be found in animal products, other agricultural products, and the agricultural environment [4]. Such contaminants in processed beef pose a serious threat to human health and can harm kidney and liver functions [4]. Beta-lactam antibiotics such as AMX have a stable chemical structure, high levels of toxicity, and slow rates of biodegradation [2]. They can therefore readily be discharged into the environment through wastewater from food and livestock production, human excretion, hospital wastewater discharge, and poor wastewater treatment [5]. Considering these, the monitoring of antibiotics such as AMX is very important.

Multiple analytical methods have been used to detect AMX, primarily surface plasmon resonance, chromatography, capillary electrophoresis, liquid chromatography coupled to tandem mass spectrometry (LC-MS-MS), spectrofluorometric and microbiological methods, enzymatic quantification, fluorescence, and spectrophotometry [2,3,6]. There is a need for simpler, less expensive, quicker, more sensitive, and more selective amoxicillin determination methods, because most current methods need time-consuming and expensive sample pre-treatment procedures [2]. Due to their benefits, including low cost, easy operation, quick measurement, and strong sensitivity and selectivity, electrochemical techniques have been used extensively in the study of antibiotics in recent decades. Electrochemical methods can also be used to quickly test for pollution on-site [5].

In the electrochemical approach, the reduction-oxidation reactions of analytes appear on the surface of the working electrode, which is a very important part of the analytical measurement. Therefore, in an effort to improve the analyte signal, scientists have

attempted to modify the electrode surface using cutting-edge techniques [5]. Most investigations on the electrochemical detection of amoxicillin in the literature are based on metallic nanoparticles combined with CNTs and graphene to produce various geometries and stacking arrangements [6].

According to the literature [7], the chemical stability of the oxides and surface OH bonds enables the covalent grafting of probe molecules in sensor applications. An example of an oxide used for AMX detection is TiO_2 [7]. Another oxide, ZnO, has generated a great deal of interest because of its admirable qualities, including inexpensive cost, great abundance, excellent catalytic activity against biological and chemical species, and antifouling characteristics [8–10]. ZnO nanoparticles also offer unique physical characteristics, including high electron mobility, a tunable band position, high chemical and thermal stability, and non-toxicity [11]. ZnO is a metal oxide semiconductor with a straight and wide band gap. Its hexagonal wurtzite crystal structure makes a variety of micro- and nanostructured materials easy to produce, including tubes, combs, and rods [8].

Various techniques can be used to create zinc oxide nanoparticles, one of them being microfluidic reactor-based synthesis [12–14]. Chemical processes including hydrothermal, sol-gel, and microemulsion, as well as physical methods such as ball milling, physical vapor deposition, and laser ablation, were also used for the synthesis of ZnO nanoparticles [15]. Biological (green) synthesis techniques are also included among the conventional methods. Various efforts have been made to create ZnO NPs from various green sources, including bacteria, fungi, algae, plants, and others [16].

Recently, ZnO nanostructures have been prepared starting from silk fibroin from silkworm *Bombyx Mori* cocoons [17]. Fibroin is a highly adaptable biopolymer that has enabled the development of a diverse range of materials whose properties and architectures may be tailored to meet specific application requirements [18]. Additionally, the *B. mori* silkworm is practical for industrial-scale breeding, making it simple to obtain silkworms and their silk, and exhibits strong biocompatibility and biodegradability [19]. It contains in situ active sites for the anchoring of a zinc nitrate—ZnO—precursor [17]. The mechanical stability, flexible biomimetic form, and biocompatibility of silk fibroin fibers were carried over into the as-prepared nanostructures [17].

This paper proposes a new electrochemical device based on ZnO nanostructures derived from a natural compound named silk fibroin. These nanostructures were incorporated into a Nafion polymer matrix. Some characteristics, such as drying time and concentration, were discovered to be crucial in the modification of a glassy carbon (GC) electrode. This type of modified electrode was proven to be useful for AMX electrochemical detection.

2. Materials and Methods

2.1. Preparation of ZnO

First, *Bombyx Mori* cocoons from a local farmer were used; the larvae were extracted from the cocoons, and they were cut into small pieces. In a 2 L Berzelius beaker, ultrapure water (obtained with a Millipore Direct-Q UV3 water filtration system) was brought to a boil (100 °C) on a thermostatic hot plate (Stuart, model UC152) and sodium carbonate (anhydrous Na_2CO_3 , 99.9%, Sigma Aldrich, Poznań, Poland) was added to 0.02 M. Boiling time was 30 min. In the last stage, the fibroin was rinsed with ultrapure water under magnetic stirring. The operation was repeated 2–3 times to remove the sodium carbonate and sericin dissolved in this solution. The silk fibroin (SF) that was produced in this way was left to dry at room temperature for 24 h.

Dried silk fibroin was then mixed with a solution of 1.462 g of $\text{Zn}(\text{NO}_3)_2 \cdot 6\text{H}_2\text{O}$ (99% metal basis, Alpha Aesar, Kandel, Germany) in 40 mL of a 1:1 distilled water : ethanol mixture at room temperature for 12 h. The $\text{Zn}(\text{NO}_3)_2$ -soaked fibroin was subjected to thermal treatment for 1 h at 200 °C, followed by 6 h at 600 °C, in a muffle furnace (LEF-1035, Daihan Labtech, Namyangju-city, Korea). This step led to the burning of fibroin and the crystallization of ZnO.

2.2. Preparation of Modified Glassy Carbon Electrodes

Glassy carbon (GC) electrodes (3 mm, Metrohm, Bucharest, Romania) were mirror-polished on polishing cloth (PRESI) with 1 μm diamond paste and 0.3 μm alumina slurry, followed by ultrasonic treatment in ultrapure water for 10 min.

Next, 25 μL Nafion solution (20 % in lower aliphatic alcohol and water from Sigma Aldrich, St Louis, Missouri, USA) was diluted to 1 mL with 0.1 M phosphate buffer solution (PBS) with pH 7. PBS was prepared from 0.2 M stock aqueous solutions of K_2HPO_4 and KH_2PO_4 . The purity of both was 98% and they were acquired from Sigma Aldrich. After cleaning the GC electrode, 3 μL of this solution was dripped onto the surface and it was left to dry. This electrode will be known as GC/Nafion.

In the meantime, 10 mg of ZnO nanostructure was added to a diluted Nafion solution in PBS, and the resulting mixture was ultrasonicated for 1 h. Then, 6 μL or 9 μL (in 3 μL portions) of the ZnO nanoparticles and Nafion solution was drop-casted onto the surface of the cleaned GC electrode with a micropipette. The electrode prepared with 6 μL and a drying time of 1 h was named GC/Nafion/ZnO 6 (1 h), the one prepared with 6 μL and a drying time of 24 h was named GC/Nafion/ZnO 6, and the last one prepared with 9 μL and a drying time of 24 h was named GC/Nafion/ZnO 9.

2.3. ZnO Structures and Modified Electrode Characterization

The modified electrode and the resulting ZnO structures were characterized using a Thermo Fisher Scientific Quanta 650 FEG Scanning Electron Microscope (SEM, Hillsborough, CA, USA), which features ESEM technology and high-resolution scanning, equipped with a Bruker energy-dispersive X-ray system (EDX) for chemical analysis.

A Perkin Elmer Spectrum 100 ATR FT-IR (Perkin Elmer, Waltham, MA, USA) was used to record the Fourier transform infrared spectrum (FTIR). Four sequential scans were used to record between 4000 and 600 cm^{-1} . The corresponding program was used to process spectra acquired at a resolution of 4 cm^{-1} , performing background correction and smoothing.

The crystalline phases and their structures were identified using a Shimadzu X-ray diffraction (XRD) 6000 diffractometer with Ni-filtered Cu K radiation ($\lambda = 0.154 \text{ nm}$), 2θ , varying between 10° and 70° .

2.4. Amoxicillin Detection

Two electrochemical methods were used for amoxicillin detection: cyclic voltammetry (CV) and DPV. Experiments were carried out in a single-compartment electrochemical cell, in a solution of PBS Ph = 7. Three electrodes were connected to a potentiostat/galvanostat (Autolab 302 N, Metrohm, Barendrecht, Nederland): a GC working electrode, an AG/AgCl 3 M KCl reference electrode (Metrohm, Bucharest, Romania), and a Pt rod (Metrohm, Bucharest, Romania). For CV measurements, the scan rate was 25 mV/s between 0.3 and 1.3 V with 0.02 V steps. DPV was recorded between 0.7 and 1.2 V with a 50 mV modulation amplitude and 20 mV/s scan rate. In addition, 0.1 M PBS pH 7 prepared from 0.2 M stock aqueous solutions of K_2HPO_4 and KH_2PO_4 (Sigma Aldrich, St Louis, Missouri, USA) with or without amoxicillin was employed as the electrolyte.

3. Results

3.1. Modified Electrode Characterization

Prepared ZnO structures and modified GC electrodes were subjected to SEM analysis and the obtained images are presented in Figure 1. In Figure 1a,b, it can be observed that the ZnO structures had a fibrous morphology with diameters between 1 and 2 μm .

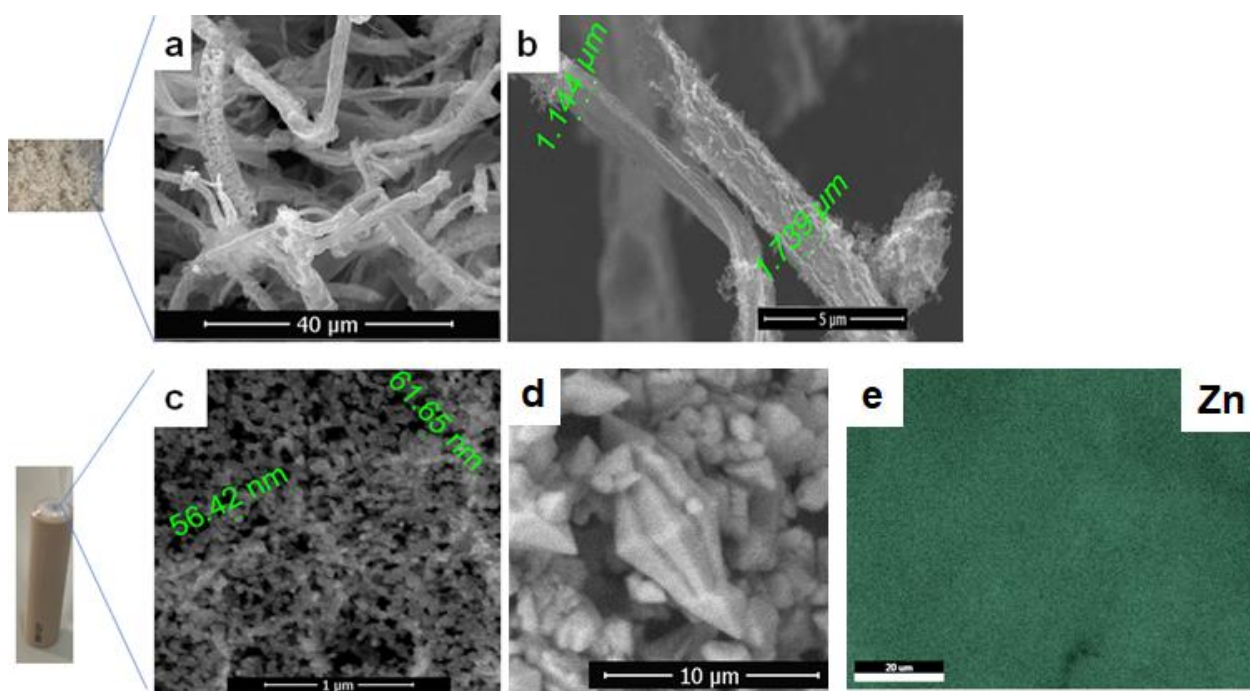


Figure 1. SEM images of obtained ZnO nanostructures (a,b) and modified GC/Nafion ZnO 6 electrode (c,d). EDS mapping of Zn from GC/Nafion ZnO 6 electrode (e).

ZnO structures were subjected to 1 h ultrasonic treatment before depositing on GC. In Figure 1c,d, there are corresponding top-view SEM images of the GC/Nafion ZnO 6 electrode. It is visible that ZnO was embedded in the Nafion matrix as nanoparticles with uniform distribution.

According to the elemental EDS mapping (Figure 1e), the polymer matrix contributed to the homogeneous dispersion of the ZnO nanoparticles without agglomeration. The uniform Zn distribution appeared on the entire surface of the electrode, as can be seen in Figure 1e, in a percentage of 15%, which helped to ensure sensor reproducibility. The Nafion matrix, with its antifouling qualities, was successfully used for nanoparticle dispersion, which led to a greater specific surface area at the electrode surface. Moreover, 51% oxygen was found, a part of the percentage being a component of Nafion and the other part associated with ZnO.

Figure 2a shows the FT-IR spectra recorded for zinc oxide structures deposited on fibroin templates compared to the spectrum recorded for silk fibroin. Thus, in the spectrum of fibroin, the peaks specific to the β -sheet structure can be observed: 1511 cm^{-1} and 1621 cm^{-1} . In the spectra of the zinc oxide nanostructures, the absorption peak at 3500 cm^{-1} , characteristic of the stretching vibration of the -OH group, can be observed. The absorption peaks at 2300 cm^{-1} and 2400 cm^{-1} are attributed to the CO_2 group, and the absorption peak at 1416 cm^{-1} is attributed to the C-C stretching vibration. The absorption band formed at 995 cm^{-1} is attributed to ZnO. These bands are consistent with data found in the literature [11,20].

In Figure 2b, the spectra obtained for zinc oxide structures obtained on the fibroin template and for the glassy carbon-modified electrode GC/Nafion/ZnO 6 are presented. In the GC/Nafion/ZnO 6 spectrum, we can observe -OH stretching vibration at 3336 cm^{-1} corresponding to adsorbed water. The peak recorded at 1005 cm^{-1} is due to S-O symmetric stretching, the band obtained at 1148 cm^{-1} is due to symmetric stretching of C-F, and the band obtained at 1215 cm^{-1} is due to the asymmetric C-F stretching. The peak obtained at 1005 cm^{-1} is attributed to the S-O group [21]. The peak at 988 cm^{-1} corresponding to ZnO [11] is covered by the much larger peak specific to Nafion. The band obtained at 637 cm^{-1} is attributed to the stretching of the C-S group from the Nafion structure [21].

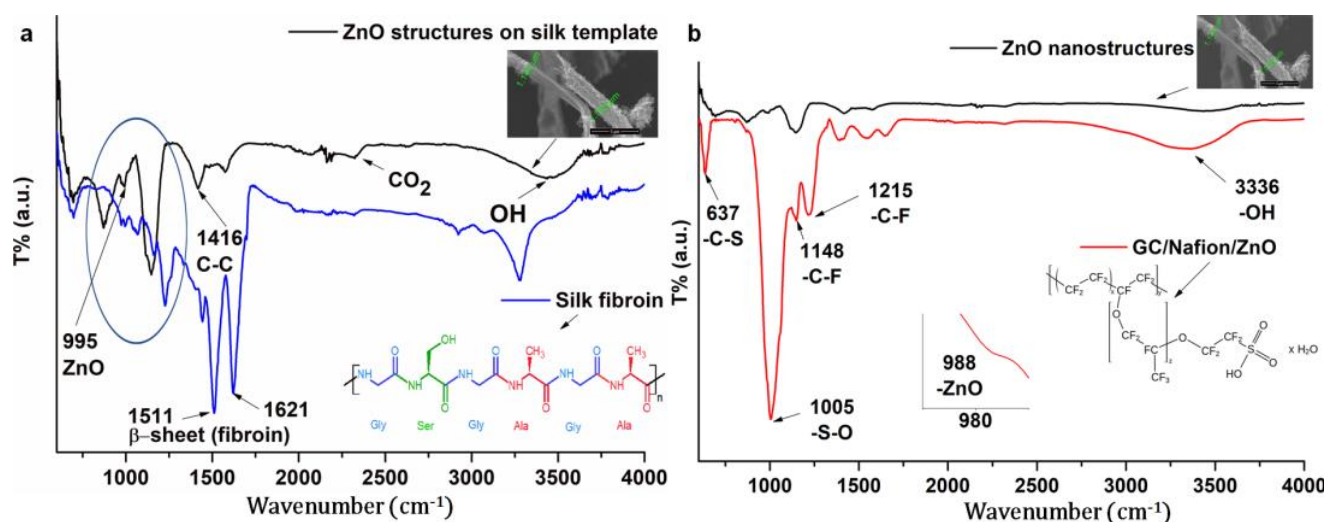


Figure 2. FT-IR spectra: (a) comparison between SF and ZnO structures on SF template and (b) comparison between ZnO nanostructures and GC/Nafion/ZnO 6.

The quality of the crystals and the orientation of the synthesized ZnO nanoparticles were studied using X-ray diffraction (XRD), and the patterns are represented in Figure 3. The sharp and narrow peaks demonstrate the sample's high crystallinity. By comparison with the data from JCPDS card No. 89-7102, all the XRD peaks are very well correlated with the hexagonal phase (wurtzite structure), with no evidence of a secondary phase. The first three peaks, defined in Table 1, were utilized to calculate particle sizes using the Scherrer equation:

$$D = \frac{k\lambda}{\beta \cos \theta} \quad (1)$$

where D is the crystallite size, $k = 0.9$ (Scherrer constant); λ is the light wavelength utilized for diffraction, which is equal to 1.54 \AA ; β is the full width at half maximum (FWHM) of the diffraction peak, and θ is the reflection angle (Bragg's angle).

The peaks of the ZnO nanostructures match the hexagonal wurtzite structure of zinc oxide. The Miller indices of the ZnO hexagonal phase's typical peaks, presented in Figure 3, are (100), (002), (101), (102), (110), (103), and (112). The average size of crystallites was 37 nm.

3.2. Selecting Proper Voltammetric Method for AMX Detection

The first tested method was cyclic voltammetry. CV curves were obtained in phosphate buffer solution and phosphate buffer with a high concentration of amoxicillin ($100 \mu\text{M}$). They are presented in Figure 4.

The unmodified GC electrode (Figure 4a) and GC/Nafion/ZnO 6 (Figure 4c) gave a signal in the presence of amoxicillin, while the GC electrode on which only the Nafion polymer was deposited (Figure 4b) did not show a signal in the presence of amoxicillin. The current values recorded for GC/Nafion are much lower compared to those recorded for GC.

Further, differential pulse voltammetry was used. The DPV curves corresponding to the GC and GC/Nafion/ZnO 6 (1 h) in phosphate buffer solution and phosphate buffer with amoxicillin $100 \mu\text{M}$ are shown in Figure 5. It is observed that a signal can be obtained in the presence of amoxicillin with the unmodified electrode. With the help of the modified electrode, a much better signal is obtained, the peak current being of the order of $8.2 \times 10^{-8} \text{ A}$, compared to $4.4 \times 10^{-8} \text{ A}$ in the case of GC.

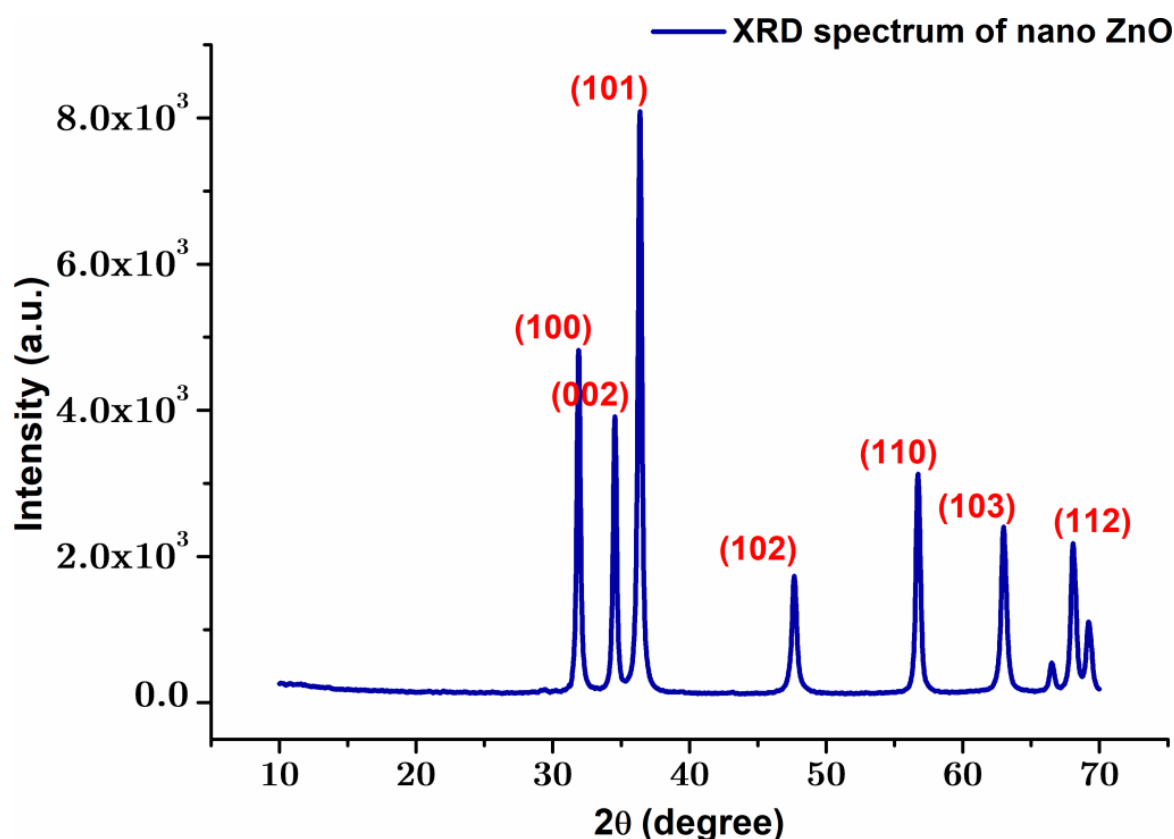


Figure 3. The X-ray diffraction (XRD) pattern of ZnO nanostructures prepared on silk fibroin template.

Table 1. The first three peaks obtained from XRD spectrum.

No.	2-Theta [θ]	d [\AA]	FWHM [θ]	Crystallite Size [nm]	Phase Name
1	31.4815	2.83945	0.1528	54	ZnO (100)
2	34.5518	2.59384	0.2720	30	ZnO (002)
3	36.3804	2.46755	0.2991	27	ZnO (101)

The drying time was increased from 1 h to 24 h and the obtained DPV curves are presented in Figure 6b. Consecutive scans were again performed in 100 μM AMX solution. It is observed that the signal, with the peak at 0.9 V, suffers a slight drop but is more stable.

3.3. Improving the Electrode Signal for AMX Detection

In order to improve the signal, an electrode with a higher concentration of Nafion + ZnO, namely GC/Nafion/ZnO 9, was prepared. The signal obtained in DPV with GC/Nafion/ZnO 6 was compared to the one obtained with GC/Nafion/ZnO 9, with the results being presented in Figure 7. The drying time was 24 h for both electrodes. The obtained peak height was greatly improved, from 6.8×10^{-8} A to 1.46×10^{-7} A.

To check the electrode stability, a series of three consecutive scans were performed in the 100 μM AMX solution in PBS with the GC/Nafion/ZnO 6 electrode (1 h). It was observed (Figure 6a) that the signal gradually decreased, with a very large difference between scans 1 and 3.

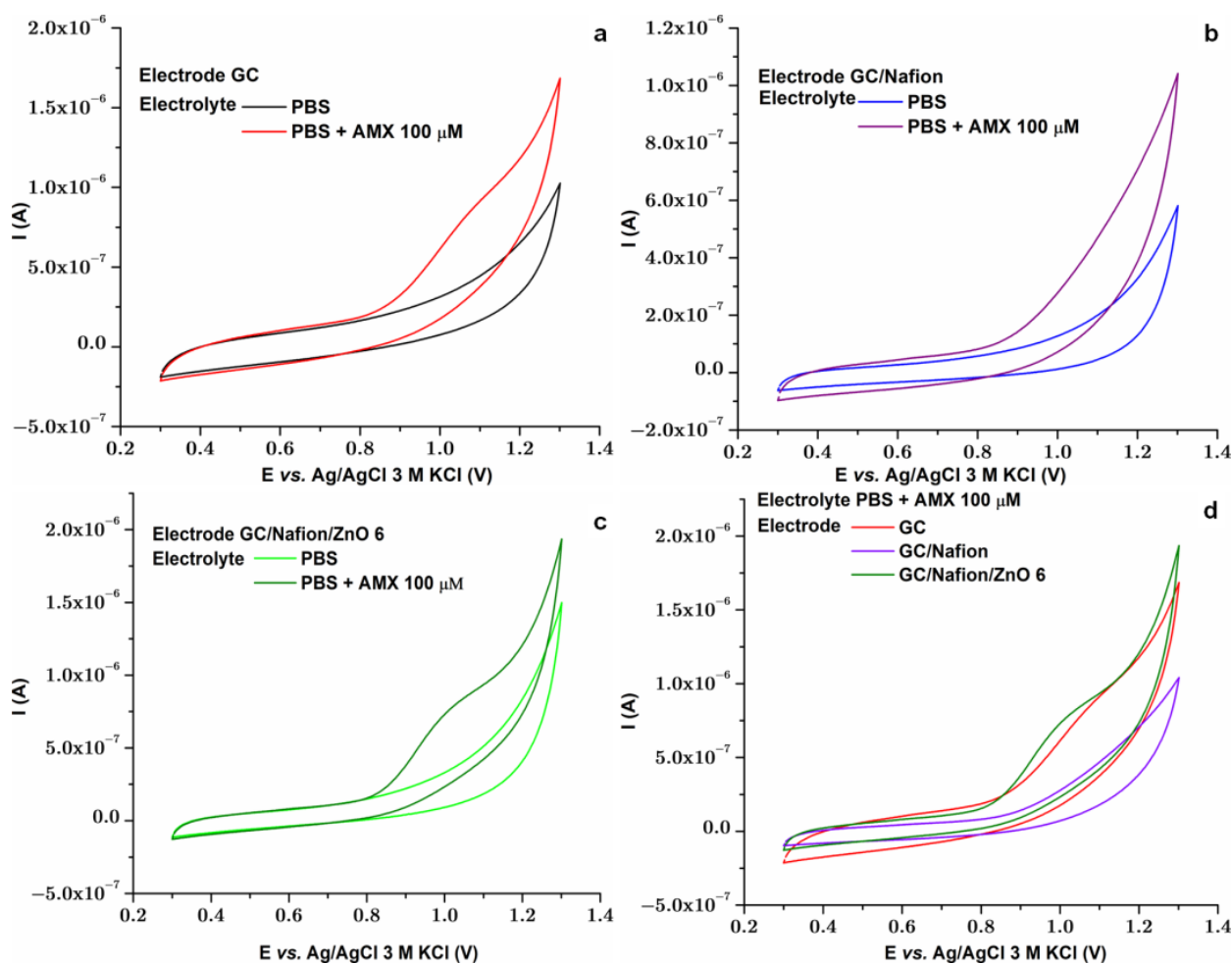


Figure 4. Cyclic voltammograms recorded in PBS and PBS + AMX 100 μM corresponding to (a) GC electrode, (b) GC/Nafion electrode, (c) GC/Nafion/ZnO 6, (d) GC/Nafion, and GC/Nafion/ZnO 6 compared with an uncoated GC electrode.

The stability of the signal was also checked for this electrode. It is observed from Figure 8a that the signal is stable for three successive scans (scan 1–3). The electrode was tested again after one week (Figure 8a, scans 4–6) and the signal decreased by 8%. It was also checked whether this last method of electrode modification could be reproduced. Thus, two similar GC/Nafion_ZnO 9 electrodes were prepared. Scans were made in freshly prepared 80 μM amoxicillin solution, with the results being presented in Figure 8b. It is observed that the obtained signal is similar.

3.4. Calibration Curve

To obtain the calibration curve, AMX solutions in PBS with concentrations between 5 and 110 μM were prepared. An increase in the peak height corresponding to the increase in the concentration of amoxicillin is observed in Figure 9b. The AMX redox reaction (Figure 9a) on the GC/Nafion/ZnO 9 electrode leads to a calibration curve with good linearity, r^2 being 0.998, as can be observed in the Figure 9b inset.

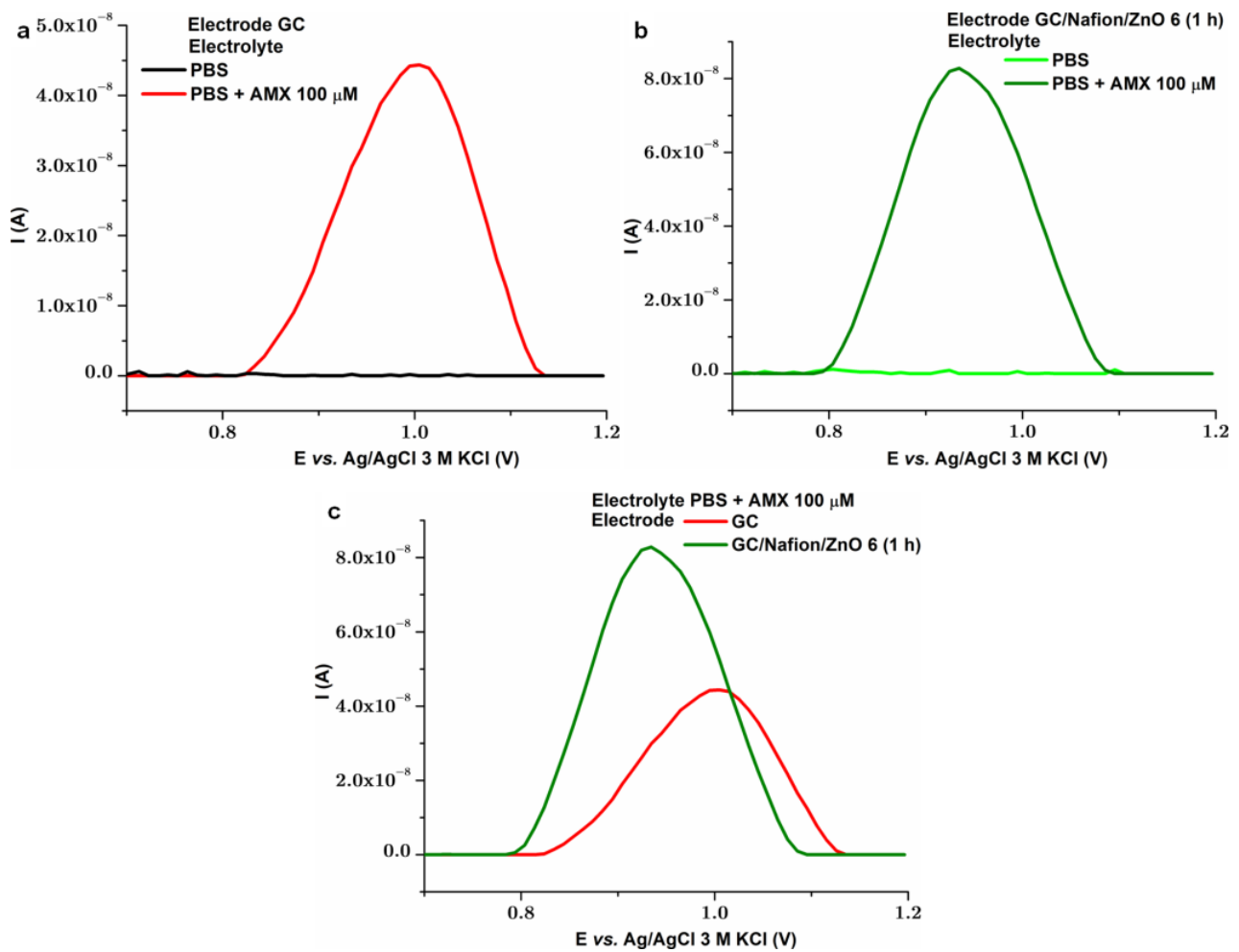


Figure 5. DPV curves corresponding to (a) GC in PBS and PBS with AMX 100 μ M, (b) GC/Nafion/ZnO 6 (1 h) in PBS and PBS with AMX 100 μ M and (c) comparison between GC and GC/Nafion/ZnO 6 (1 h) in PBS with AMX 100 μ M.

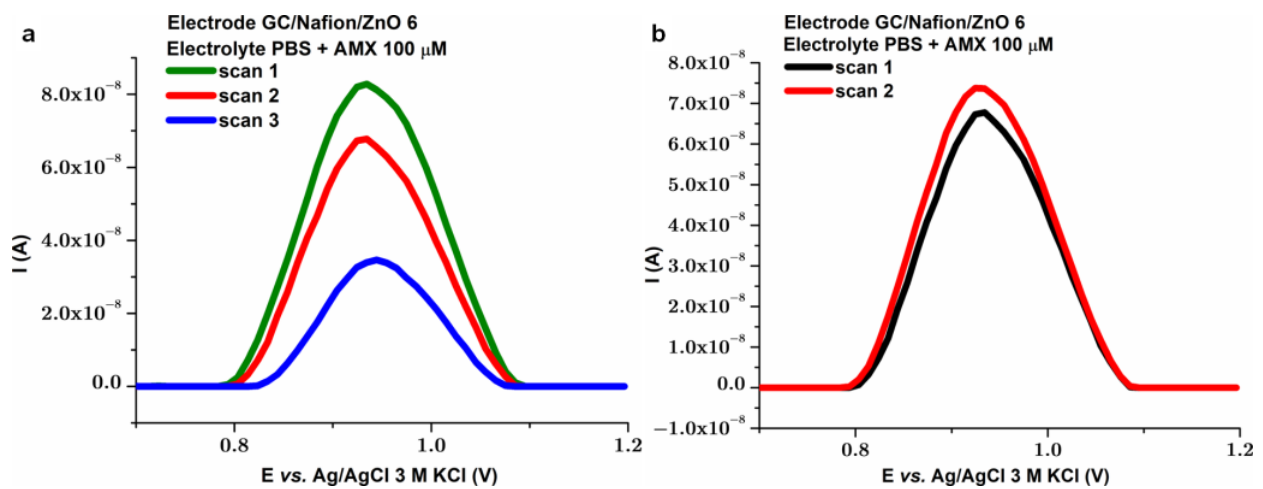


Figure 6. Differential pulse voltammetry curves in PBS with AMX 100 μ M consecutive scans using GC/Nafion ZnO 6 electrode with (a) 1 h drying time, (b) 24 h drying time.

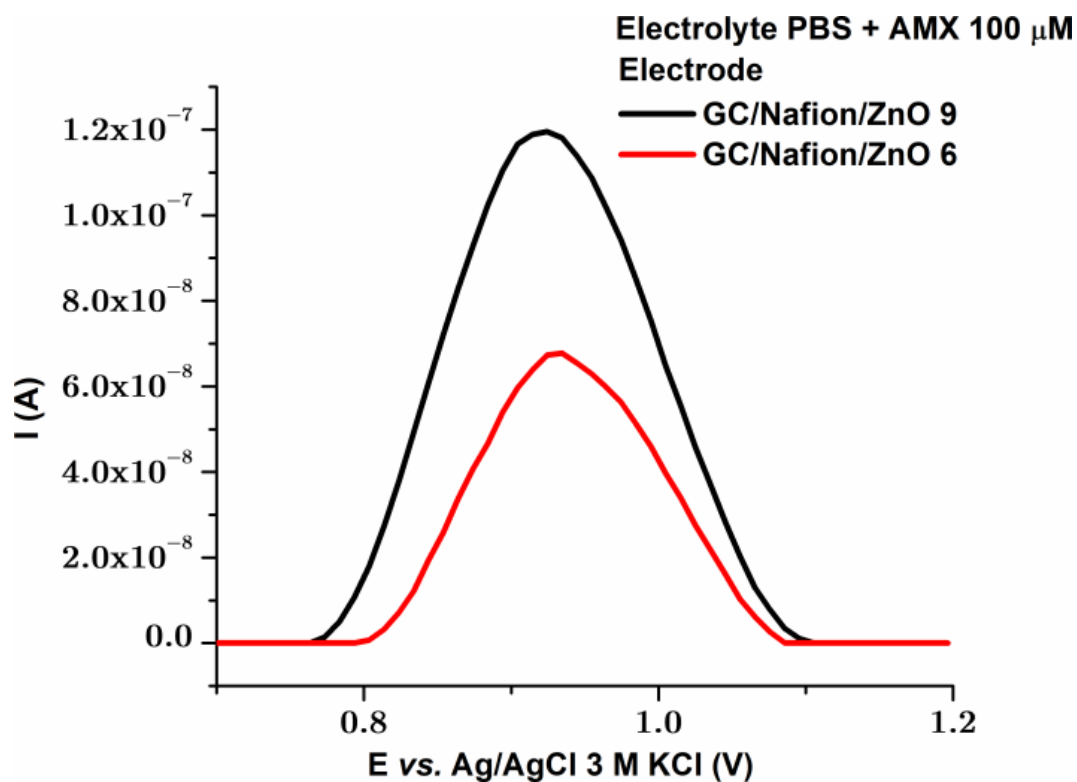


Figure 7. DPV curves in PBS solution + AMX 100 μ M corresponding to GC/Nafion/ZnO 9 and GC/Nafion/ZnO 6.

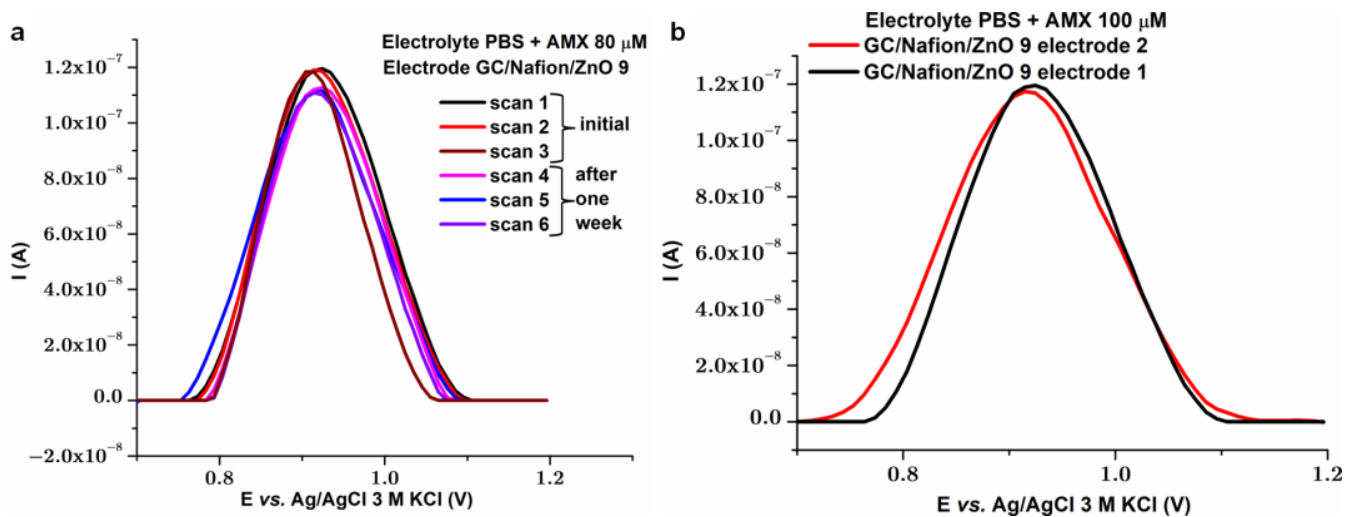


Figure 8. DPV curves in PBS + AMX 80 μ M recorded with GC/Nafion/ZnO 9: (a) consecutive scans with the same electrode, (b) scans recorded with two freshly prepared electrodes.

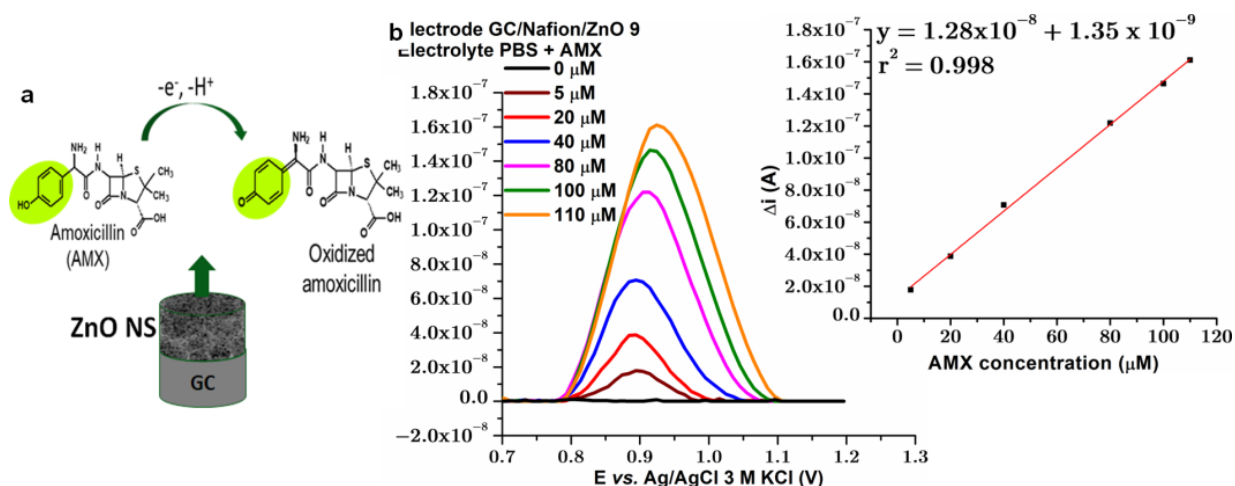


Figure 9. (a) Redox reaction of AMX; (b) DPV curves in PBS + AMX 6 different concentrations; and calibration curve using GC/Nafion/ZnO 9 electrode.

4. Discussion

4.1. ZnO Structures and Electrode Modification

To create ZnO nanostructures, the template method was used in different studies [22]. In this method, nanostructures are grown through the pores or channels of a template using a nucleation and growth process, using a template with a preset size and shape. Hard and soft templates are examples of the two different types of templates used for ZnO synthesis. A soft template is made up of flexible polymers and biomolecular and single molecular-based templates, whereas a hard template often consists of CNT and porous alumina [22]. In this study, flexible biopolymer silk fibroin was used. The ZnO-prepared structures have a fibrous morphology (Figure 1) and larger specific surface area, as can be seen from the SEM images. ZnO structures prepared in a similar manner were reported to have a wurtzite crystallite structure [17]. The wurtzite's tetrahedral atom coordination leads to a non-centrosymmetric crystal structure with polar Zn^{2+} and O_2 surfaces, which gives rise to piezoelectric qualities that make it possible to use these nanostructures in mechanical actuators and sensing technology [23].

In the scientific literature, two types of conformations specific to silk fibroin are specified: β -sheets—with a crystalline, organized, hydrophobic domain—and a random coil/ α -helix domain specific to amides I, II, and III. For the random coil/ α -helix conformation, the corresponding peaks are found in the ranges of $1638\text{--}1660\text{ cm}^{-1}$, $1536\text{--}1545\text{ cm}^{-1}$, and 1235 cm^{-1} for amides I, II, and III, respectively. In the case of the crystal conformation, the β -sheet, the corresponding peaks are found in the ranges of $1616\text{--}1637\text{ cm}^{-1}$, $1513\text{--}1525\text{ cm}^{-1}$, and 1265 cm^{-1} for amides I, II, and III, respectively [20]. From the obtained spectra shown in Figure 2a, our prepared silk fibroin has a β -sheet configuration.

For ZnO structures, the silk fibroin template was removed after thermal treatment at $600\text{ }^\circ\text{C}$ and the $\text{Zn}(\text{NO}_3)_2$ was decomposed into ZnO. As can be seen from Figure 2a, in the FT-IR spectra, peaks specific to fibroin are not present in the spectra corresponding to ZnO structures.

These ZnO structures were successfully embedded in the Nafion polymer matrix, as can be seen from Figure 2b. Nafion is a well-known ionic polymer with benefits of good ionic conductivity, cation selectivity, chemical inertness, and thermal stability. It is made up of sulfonate groups and a stable hydrophobic polytetrafluoroethylene backbone. It adheres well to the majority of electrode surfaces and can prevent them from fouling or degrading [24]. Nafion polymer was selected because it helps in enhancing the stability of the sensor; water can pass through Nafion quite easily, and it can withstand chemical attacks [25,26]. It helps in increasing ion exchange during the oxidation reduction process with its ion-exchanging abilities.

From the XRD pattern (Figure 3), the strongest line in the ZnO sample under examination falls along the (1 0 1) plane. Additionally, the diffraction peaks are narrow and intense, this being a sign of a well-formed crystalline structure, in the nanoscale range, confirmed by Scherrer equation calculations. Pure ZnO nanoparticles having a hexagonal wurtzite phase were created, because no diffraction peaks matching other ZnO phases or organic compounds were found. This could be proof of the successful burning of silk fibroin by thermal treatment.

4.2. Amoxicillin Electrochemical Detection

For the sensitive detection of organic compounds, including medicines and related substances, in pharmaceutical samples and biological fluids, electrochemical techniques have proven to be excellent methods [27]. Among all electrochemical techniques utilized for AMX detection, there are several voltametric approaches, such as linear voltammetry, CV, square wave voltammetry (SWV), and DPV [28]. For example, CV was used to demonstrate the catalytic oxidation of AMX using a chemically modified nickel-based (Ni(II)-curcumin) modified carbon paste electrode by Reza Ojani and coworkers [27]. According to their experimental findings, the amoxicillin catalytic oxidation current at this electrode can be utilized to assess the amount of AMX in aqueous solution, allowing for the achievement of a detection limit and linear dynamic range that are suitable [27].

Adding Nafion to the GC surface leads to a current decrease, and ZnO nanostructures' incorporation into Nafion leads to a slight improvement, but this is not sufficient. In our case, for the GC/Nafion/ZnO 6 complex electrode, the highest signal is found in the presence of AMX 100 μM , as can be seen in Figure 4. With our proposed modified electrode based on Nafion/ZnO, it can be concluded that CV is not sensitive enough to be used as an electrochemical method for the detection of amoxicillin.

Another tested method was DPV. In the first experiment, presented in Figure 5, we used GC/Nafion/ZnO 6 (1 h) to decrease the electrode preparation time. It seems that DPV is suitable for AMX detection with the proposed modified electrode, leading to an almost two-fold improvement in the signal.

When consecutive scans were performed with GC/Nafion/ZnO 6 (1 h), the signal was not stable (Figure 6a); one possible explanation could be that the Nafion film was not sufficiently dried. It is possible that 1 h is not sufficient time for the PBS solvent used for Nafion solution preparation to be evaporated, leading to ZnO nanostructures' detachment from the electrode surface between scans.

When the drying time of the electrode is increased to 24 h (Figure 6b), the signal is more stable, so, in all further experiments, we used a 24 h drying time for electrode preparation.

According to the results presented in Figure 7, another important parameter for this modified electrode is the concentration. Upon increasing the concentration from 6 μL of solution to 9 μL , the peak height was doubled.

The GC/Nafion/ZnO 9 electrode's stability during three consecutive scans is presented in Figure 8. The electrode prepared by this method gives a stable signal in the presence of AMX. After one week, a slight decrease in peak height is observed, but there is not a large difference during three consecutive scans. Reproducibility was tested (Figure 8) and it could be concluded that the modification method can be reproduced.

With the proposed modified electrode, a calibration curve can be obtained (Figure 9). With the Excel program, the LOD and LOQ were calculated—respectively, the limit of detection and the limit of quantification—according to the linear regression method described in the literature [29]. The LOD was 0.02 μM and LOQ 0.05 μM .

Comparing the created sensor's sensitivity to some of the existing reported voltametric sensors, as presented in Table 2, GC/Nafion/ZnO was more sensitive. The linear response range is comparable to other electrochemical sensors' linear ranges. Another benefit of the created sensor is the ease of its fabrication and the use of nanocomposite ZnO based on fibroin, which does not affect the environment, which is significant considering the principles of green chemistry.

Table 2. Analytical characteristics evaluated for amoxicillin electrochemical sensors.

WE ¹	Transduction Method	Linear Range (μM)	LOD (μM)	Reference
Treated GPE ²	SWV	1–80	0.2 μM	[28]
TiO ₂ /CMK/AuNPs/ Nafion/GCE ³	CV	0.5–2.5 2.5–133.0	0.3	[30]
ZnO NRs/gold/glass electrode ⁴	CV	5.0–2.5	1.9	[31]
MWCNT/GCE ⁵	CV	0.6–8	0.2	[32]
Poly-4-vinylpyridine/CPE ⁶	CV	-	8	[33]
[VO(Salen)]/CPE ⁷	DPV	18.3–35.5	16.6	[34]
FeCr ₂ O ₄ /MWCNTs /GCE ⁸	DPV	0.1–10.0 10.0–70.0	0.05	[35]
CILE ⁹	CV	5.0–400	0.8	[36]
ZnO/Nafion/GC	DPV	5–110	0.02	This work

¹ Working electrode. ² Graphite pencil mechanically polished. ³ Titanium dioxide/mesoporous carbon CMK-3-type/gold nanoparticles/Nafion on glassy carbon electrode. ⁴ Zinc oxide nanorod/gold/glass electrode. ⁵ Multiwalled carbon nanotube modified glassy carbon electrode. ⁶ Carbon paste electrode modified with poly-4-vinylpyridine. ⁷ Carbon paste electrode modified with [N,N-ethylenebis(salicylideneamino)]oxovanadium. ⁸ Nanoparticle-decorated multiwall carbon nanotubes on glassy carbon electrode. ⁹ Carbon ionic liquid electrode.

5. Conclusions

A new electrochemical sensor based on ZnO nanostructures grown in a natural silk fibroin matrix was obtained. The ZnO nanostructures, with high porosity and a fibrillar shape, were deposited on the glassy carbon electrode surface by incorporation into a Nafion polymer matrix.

Glassy carbon surface modification was highlighted by scanning electron microscopy, energy-dispersive X-ray spectroscopy, X-ray diffraction, and Fourier-transform infrared spectroscopy analysis. The ZnO structures prepared on the silk fibroin template had a fibrous morphology and their diameters ranged from 1 to 2 μm . X-ray diffraction revealed a hexagonal wurtzite phase. The size of crystallites was around 37 nm. X-ray diffraction and Fourier-transform infrared spectroscopy showed that silk fibroin was successfully burned by thermal treatment. ZnO was then distributed uniformly as nanoparticles within the Nafion matrix on the glassy carbon electrode's surface.

The new GC/Nafion/ZnO electrode, with good stability, was successfully used for AMX electrochemical detection, with an LOD of 0.02 μM , which was better than or comparable to values reported in other papers. The built-in standard calibration has a high degree of correlation.

Measurements in solutions containing different antibiotics will be performed to test the AMX selectivity.

Author Contributions: Conceptualization, C.D. and C.P.; methodology, C.D. and C.P.; software, C.D., A.C., and A.D.; validation, C.D., A.C., A.D., and C.P.; formal analysis, C.D., A.C., and A.D.; investigation, A.D. and C.D.; resources, C.D. and C.P.; data curation, C.D.; writing—original draft preparation, C.D.; writing—review and editing, C.D., A.C., and C.P.; supervision, C.P.; project administration, C.D. All authors have read and agreed to the published version of the manuscript.

Funding: This research received no external funding.

Informed Consent Statement: Not applicable.

Data Availability Statement: Not applicable here.

Conflicts of Interest: The authors declare no conflict of interest.

References

1. Wong, A.; Santos, A.M.; Cincotto, F.H.; Moraes, F.C.; Fatibello-Filho, O.; Sotomayor, M.D.P.T. A new electrochemical platform based on low-cost nanomaterials for sensitive detection of the amoxicillin antibiotic in different matrices. *Talanta* **2020**, *206*, 120252. [[CrossRef](#)] [[PubMed](#)]
2. Essousi, H.; Barhoumi, H.; Karastogianni, S.; Girousi, S.T. An Electrochemical Sensor Based on Reduced Graphene Oxide, Gold Nanoparticles and Molecular Imprinted Over-oxidized Polypyrrole for Amoxicillin Determination. *Electroanalysis* **2020**, *32*, 1546–1558. [[CrossRef](#)]
3. Norouzi, B.; Mirkazemi, T. Electrochemical sensor for amoxicillin using Cu/poly (o-toluidine) (sodium dodecyl sulfate) modified carbon paste electrode. *Russ. J. Electrochem.* **2016**, *52*, 37–45. [[CrossRef](#)]
4. Li, S.; Ma, X.; Pang, C.; Li, H.; Liu, C.; Xu, Z.; Luo, J.; Yang, Y. Novel molecularly imprinted amoxicillin sensor based on a dual recognition and dual detection strategy. *Anal. Chim. Acta* **2020**, *1127*, 69–78. [[CrossRef](#)] [[PubMed](#)]
5. Pham, T.H.Y.; Mai, T.T.; Nguyen, H.A.; Chu, T.T.H.; Vu, T.T.H.; Le, Q.H. Voltammetric Determination of Amoxicillin Using a Reduced Graphite Oxide Nanosheet Electrode. *J. Anal. Methods Chem.* **2021**, *2021*, 8823452. [[CrossRef](#)]
6. Hrioua, A.; Loudiki, A.; Farahi, A.; Bakasse, M.; Lahrich, S.; Saqrane, S.; El Mhammedi, M.A. Recent advances in electrochemical sensors for amoxicillin detection in biological and environmental samples. *Bioelectrochemistry* **2021**, *137*, 107687. [[CrossRef](#)]
7. Song, J.; Huang, M.; Jiang, N.; Zheng, S.; Mu, T.; Meng, L.; Liu, Y.; Liu, J.; Chen, G. Ultrasensitive detection of amoxicillin by TiO₂-g-C₃N₄@AuNPs impedimetric aptasensor: Fabrication, optimization, and mechanism. *J. Hazard. Mater.* **2020**, *391*, 122024. [[CrossRef](#)]
8. Shetti, N.P.; Bukkitgar, S.D.; Reddy, K.R.; Reddy, C.V.; Aminabhavi, T.M. ZnO-based nanostructured electrodes for electrochemical sensors and biosensors in biomedical applications. *Biosens. Bioelectron.* **2019**, *141*, 111417. [[CrossRef](#)]
9. Lefatshe, K.; Muiva, C.M.; Kebaabetswe, L.P. Extraction of nanocellulose and in-situ casting of ZnO/cellulose nanocomposite with enhanced photocatalytic and antibacterial activity. *Carbohydr. Polym.* **2017**, *164*, 301–308. [[CrossRef](#)]
10. Ong, C.B.; Ng, L.Y.; Mohammad, A.W. A review of ZnO nanoparticles as solar photocatalysts: Synthesis, mechanisms and applications. *Renew. Sustain. Energy Rev.* **2018**, *81*, 536–551. [[CrossRef](#)]
11. Hoseinpour, V.; Souri, M.; Ghaemi, N.; Shakeri, A. Optimization of green synthesis of ZnO nanoparticles by *Dittrichia graveolens* (L.) aqueous extract. *Health Biotechnol. Biopharma* **2017**, *1*, 39–49. [[CrossRef](#)]
12. Jin, S.E.; Jin, H.E. Synthesis, Characterization, and Three-Dimensional Structure Generation of Zinc Oxide-Based Nanomedicine for Biomedical Applications. *Pharmaceutics* **2019**, *11*, 575. [[CrossRef](#)] [[PubMed](#)]
13. Gutul, T.; Rusu, E.; Condur, N.; Ursaki, V.; Goncarenco, E.; Vlazan, P. Preparation of poly(N-vinylpyrrolidone)-stabilized ZnO colloid nanoparticles. *Beilstein J. Nanotechnol.* **2014**, *5*, 402–406. [[CrossRef](#)] [[PubMed](#)]
14. Pan, Y.; Zuo, J.; Hou, Z.; Huang, Y.; Huang, C. Preparation of Electrochemical Sensor Based on Zinc Oxide Nanoparticles for Simultaneous Determination of AA, DA, and UA. *Front. Chem.* **2020**, *8*, 592538. [[CrossRef](#)] [[PubMed](#)]
15. Weldegebriael, G.K. Synthesis method, antibacterial and photocatalytic activity of ZnO nanoparticles for azo dyes in wastewater treatment: A review. *Inorg. Chem. Commun.* **2020**, *120*, 108140. [[CrossRef](#)]
16. Agarwal, H.; Venkat Kumar, S.; Rajeshkumar, S. A review on green synthesis of zinc oxide nanoparticles—An eco-friendly approach. *Resour. Effic. Technol.* **2017**, *3*, 406–413. [[CrossRef](#)]
17. Chen, L.; Xu, X.; Cui, F.; Qiu, Q.; Chen, X.; Xu, J. Au nanoparticles-ZnO composite nanotubes using natural silk fibroin fiber as template for electrochemical non-enzymatic sensing of hydrogen peroxide. *Anal. Biochem.* **2018**, *554*, 1–8. [[CrossRef](#)]
18. Bucciarelli, A.; Motta, A. Use of Bombyx mori silk fibroin in tissue engineering: From cocoons to medical devices, challenges, and future perspectives. *Biomater. Adv.* **2022**, *139*, 212982. [[CrossRef](#)]
19. Yao, X.; Zou, S.; Fan, S.; Niu, Q.; Zhang, Y. Bioinspired silk fibroin materials: From silk building blocks extraction and reconstruction to advanced biomedical applications. *Mater. Today Bio* **2022**, *16*, 100381. [[CrossRef](#)]
20. Park, H.J.; Lee, J.S.; Lee, O.J.; Sheikh, F.A.; Moon, B.M.; Ju, H.W.; Kim, J.-H.; Kim, D.-K.; Park, C.H. Fabrication of microporous three-dimensional scaffolds from silk fibroin for tissue engineering. *Macromol. Res.* **2014**, *22*, 592–599. [[CrossRef](#)]
21. Sigwadi, R.; Dhlamini, M.S.; Mokrani, T.; Nēmavhola, F.; Nonjola, P.F.; Msomi, P.F. The proton conductivity and mechanical properties of Nafion®/ZrP nanocomposite membrane. *Heliyon* **2019**, *5*, e02240. [[CrossRef](#)] [[PubMed](#)]
22. Bhati, V.S.; Hojamberdiev, M.; Kumar, M. Enhanced sensing performance of ZnO nanostructures-based gas sensors: A review. *Energy Rep.* **2020**, *6*, 46–62. [[CrossRef](#)]
23. Sha, R.; Basak, A.; Maity, P.C.; Badhulika, S. ZnO nano-structured based devices for chemical and optical sensing applications. *Sens. Actuators Rep.* **2022**, *4*, 100098. [[CrossRef](#)]
24. Chen, Z.; Patel, R.; Berry, J.; Keyes, C.; Satterfield, C.; Simmons, C.; Neeson, A.; Cao, X.; Wu, Q. Development of Screen-Printable Nafion Dispersion for Electrochemical Sensor. *Appl. Sci.* **2022**, *12*, 6533. [[CrossRef](#)]
25. Marie, M.; Mandal, S.; Manasreh, O. An enzymatic glucose detection sensor using ZnO nanostructure. *MRS Adv.* **2016**, *1*, 847–853. [[CrossRef](#)]
26. Mandal, S.; Marie, M.; Manasreh, O. Fabrication of an Electrochemical Sensor for Glucose Detection using ZnO Nanorods. *MRS Adv.* **2016**, *1*, 861–867. [[CrossRef](#)]
27. Ojani, R.; Raoof, J.-B.; Zamani, S. A novel voltammetric sensor for amoxicillin based on nickel–curcumin complex modified carbon paste electrode. *Bioelectrochemistry* **2012**, *85*, 44–49. [[CrossRef](#)] [[PubMed](#)]

28. Yen, P.T.H.; Anh, N.H.; Ha, V.T.T.; Hung, L.Q.; Phong, P.H.; Hien, C.T.T. Electrochemical properties of amoxicillin on an economical, simple graphite pencil electrode and the ability of the electrode in amoxicillin detection. *Vietnam. J. Chem.* **2020**, *58*, 201–205. [[CrossRef](#)]
29. Miller, J.N.; Miller, J.C. *Statistics and Chemometrics for Analytical Chemistry*; Prentice Hall/Pearson: Hoboken, NJ, USA, 2010.
30. Pollap, A.; Knihnicki, P.; Kuśtrowski, P.; Kozak, J.; Gołda-Cępa, M.; Kotarba, A.; Kochana, J. Sensitive voltammetric amoxicillin sensor based on tio2 sol modified by cmk-3-type mesoporous carbon and gold nanoparticles. *Electroanalysis* **2018**, *30*, 2386–2396. [[CrossRef](#)]
31. Hatamie, A.; Echresh, A.; Zargar, B.; Nur, O.; Willander, M. Fabrication and characterization of highly-ordered Zinc Oxide nanorods on gold/glass electrode, and its application as a voltammetric sensor. *Electrochim. Acta* **2015**, *174*, 1261–1267. [[CrossRef](#)]
32. Rezaei, B.; Damiri, S. Electrochemistry and adsorptive stripping voltammetric determination of amoxicillin on a multiwalled carbon nanotubes modified glassy carbon electrode. *Electroanal. Int. J. Devoted Fundam. Pract. Asp. Electroanal.* **2009**, *21*, 1577–1586. [[CrossRef](#)]
33. Biryol, I.; Uslu, B.; Küçükyavuz, Z. Voltammetric determination of amoxicillin using a carbon paste electrode modified with poly (4-vinyl pyridine). *STP Pharma Sci.* **1998**, *8*, 383–386.
34. Bergamini, M.F.; Teixeira, M.F.; Dockal, E.R.; Bocchi, N.; Cavaleiro, É.T. Evaluation of different voltammetric techniques in the determination of amoxicillin using a carbon paste electrode modified with [N, N'-ethylenebis (salicylideneamino)] oxovanadium (IV). *J. Electrochem. Soc.* **2006**, *153*, E94. [[CrossRef](#)]
35. Ensafi, A.A.; Allafchian, A.R.; Rezaei, B. Multiwall carbon nanotubes decorated with FeCr2O4, a new selective electrochemical sensor for amoxicillin determination. *J. Nanoparticle Res.* **2012**, *14*, 1244. [[CrossRef](#)]
36. Absalan, G.; Akhond, M.; Ershadifar, H. Highly sensitive determination and selective immobilization of amoxicillin using carbon ionic liquid electrode. *J. Solid State Electrochem.* **2015**, *19*, 2491–2499. [[CrossRef](#)]